Details of the Acyl-Enzyme Intermediate and the Oxyanion Hole in Serine Protease Catalysis†

Adam K. Whiting and Warner L. Peticolas*

Department of Chemistry, University of Oregon, Eugene, Oregon 97403

Received July 13, 1993; Revised Manuscript Received November 8, 1993®

ABSTRACT: Raman, absorbance, and kinetic measurements were used to determine how the serine protease active site feature known as the oxyanion hole interacts with an acyl-enzyme intermediate. The substrate, *p*-(dimethylamino)benzoylimidazolide (DAB-Im), was synthesized and used to prepare DAB-acyl-enzymes of wild-type (WT) and N155G subtilisin-BPN′ (the N155G mutant lacks a fully functioning oxyanion hole), α-chymotrypsin (CHT), and bovine trypsin (TRY). DAB-acyl-enzyme deacylation rate constants, k_3, were found to span a 720-fold range at pH 7.8 (DAB-WT > DAB-TRY > DAB-N155G > DAB-CHT). DAB-N155G was found to deacylate 80-fold slower than DAB-WT, indicating a 2.6 kcal/mol loss of transition-state binding energy due to this mutation. Absorbance spectra revealed strongly red-shifted absorbance λ_{max} values for all of the DAB-acyl-enzymes. The red shift was found to be 2.0 nm less in DAB-N155G, indicating that the oxyanion hole is partially responsible for this electronic perturbation of the DAB chromophore at the active site. Raman difference spectra of the DAB-acyl-enzymes measured at pH 5.0 and 8.6, with ^{18}O-labeling of the carbonyl, show that the molecular motions most perturbed by the active site are three associated with the scissile acyl bond. Most interesting is the carbonyl stretching vibration, ν(C=O), whose motion extends into the hydrolytic reaction coordinate. Comparison of the ν(C=O) of DAB-WT and DAB-N155G reveals that the oxyanion hole does indeed form a hydrogen-bonding interaction with the carbonyl oxygen, the strength of which increases at pH 8.6. Interestingly, the DAB-TRY carbonyl forms very strong hydrogen bonds, even at pH 5.0, but DAB-CHT does not, even at pH 8.6. The low-frequency (1661 cm^{-1}) ν(C=O)'s of pH 5.0 DAB-TRY and pH 8.6 DAB-WT are proposed to correspond to a tetrahedrally distorted carbonyl center like that observed in the crystal structure of guanidinobenzoyl-TRY (Mangel *et al.*, 1990). The strength of hydrogen bonding between the DAB-acyl-enzyme's carbonyl and the oxyanion hole, as gauged by the ν(C=O) frequency, was found to correlate positively with an increased deacylation rate. This correlation, as well as calculated acyl-enzyme carbonyl bond lengths, which indicate a 0.015-Å lengthening due to the oxyanion hole interaction, was found to be in good agreement with previously published resonance Raman data of α,β-unsaturated arylacryloyl-acyl-enzymes (Tonge & Carey, 1990b, 1992).

The serine proteases comprise two superfamilies of enzymes: the chymotrypsins and the subtilisins, whose function is the catalytic hydrolysis of peptide bonds (Hartley, 1970). The serine protease catalyzed hydrolysis of peptide bonds is arguably the best understood enzyme mechanism, both functionally and structurally [for reviews, see Walsh (1979) and Kossiakoff (1987)]. In addition to the well-known catalytic triad, crystal structures of α-chymotrypsin (Henderson, 1970) and subtilisin-BPN′ (Robertus *et al.*, 1972) have revealed two conserved hydrogen-bond donors known as the oxyanion hole. The oxyanion hole has been found to be a common active-site structure for all known serine proteases (Kraut, 1977), as well as two other families of catalytic triad containing enzymes: the lipases (Brady *et al.*, 1990; Winkler *et al.*, 1990) and the serine carboxypeptidases (Liao *et al.*, 1992). In most serine proteases, both of the oxyanion hole hydrogen bonds are donated by main-chain amides (one from the amide nitrogen of the catalytic serine and one from a nearby glycine amide), but in subtilisin-BPN′, one is contributed by the $N^{\delta 2}$ of an asparagine side chain (N155). Using site-directed mutagenesis, it has been possible to measure the contribution of this interaction to catalysis. A wide range of N155 mutations has been carried out which demonstrate that the oxyanion hole is essential to catalysis, contributing from 3 to 5 kcal/mol to transition-state stabilization (Wells *et al.*, 1986; Bryan *et al.*, 1986). The oxyanion hole is presumed to act only by stabilizing the high-energy tetrahedral oxyanion intermediates that reside near the transition states on the serine protease catalytic pathway.

Whereas the tetrahedral intermediate has never been observed directly, the development of chromophoric acylating agents has allowed direct spectrophotometric (Schonbaum *et al.*, 1961; Bender, 1962) and Raman (Schmidt *et al.*, 1978; MacClement *et al.*, 1981; Argade *et al.*, 1984) measurements to be made of the serine protease acyl-enzyme intermediate. Although crystal structures (Henderson, 1970) and modeling (Matthews *et al.*, 1975) of serine protease acyl-enzymes have revealed no interaction between the oxyanion hole and the acyl-enzyme intermediate, a series of resonance Raman experiments of chromophoric acyl-enzymes of α-chymotrypsin and subtilisin-BPN′ has shown that hydrogen bonding can occur (Tonge & Carey, 1990b). Furthermore, these hydrogen bonds accelerate the reaction by distorting the ground-state acyl-enzyme structure along the enzymatic pathway (Tonge & Carey, 1990b, 1992).

Previous workers have demonstrated that *p*-(dimethylamino)benzoylimidazolide (DAB-Im[1]) forms an acyl-enzyme intermediate with α-chymotrypsin that is very stable at low pH and yields good Raman difference spectra, featuring a relatively strong carbonyl stretching vibration, ν(C=O)

† Supported by NIH Grants GM 15547 and GM 33825.
® Abstract published in *Advance ACS Abstracts*, January 1, 1994.

0006-2960/94/0433-552$04.50/0

(Argade *et al.*, 1984). In this article, we describe Raman difference spectroscopic measurements of the DAB-acyl-enzyme intermediates of WT and N155G subtilisin-BPN′, α-chymotrypsin (CHT), and bovine trypsin (TRY). The N155G mutant is of particular interest as it results the loss of one of two hydrogen bonds that make up the oxyanion hole. Spectral measurements were made at both pH 5.0 and 8.6 in order to detect vibrational changes that accompany the increase in deacylation rate upon titration of the active-site histidine. Spectra were also obtained with ^{18}O-labeled carbonyl oxygens, allowing unambiguous assignment of the carbonyl stretching band, ν(C=O), as well as revealing two other strong Raman bands associated with the motions of the carbonyl. Also described are absorbance (UV–vis) and kinetic measurements of the DAB-acyl-enzymes, which allow correlations to be made between the Raman spectra, the electronic structure, and the catalytic activity. Three main questions are addressed in the interpretation of the data: (1) How does the active site affect the vibrational modes of the DAB-acyl-enzyme relative to the model compound in solution? (2) How do the vibrational motions differ among the various DAB-acyl-enzymes studied? (3) How do the Raman spectra of the DAB-acyl-enzymes correlate with known structural features and catalytic activity?

MATERIALS AND METHODS

Sources of Materials. *p*-(Dimethylamino)benzoic acid (DAB-OH) and 1,1′-carbonyldiimidazole were obtained from Aldrich and recrystallized. *p*-(dimethylamino)benzoic acid ethyl ester (DAB-OEt) was from TCI American. $H_2{}^{18}O$ was obtained from EG&G Mound Applied Technologies. α-Chymotrypsin (lot no. 128F8035), subtilisin-BPN′ (protease type VII, lot no. 71H0902), bovine trypsin (lot no. 65F-8190), and buffer salts were from Sigma Chemical Co. α-Chymotrypsin (CHT) and bovine trypsin (TRY) were used without further purification. Subtilisin-BPN′ (WT) was purified by cation-exchange chromatography on Whatman CM52 (0–300 mM NaCl gradient, pH 5.5, 10 mM MES, 5 mM $CaCl_2$) to eliminate fluorescent impurities. N155G subtilisin-BPN′ (N155G) was a gift from Dr. James Wells of Genentech, Inc., and had been purified according to published methods (Carter *et al.*, 1985).

^{18}O Labeling of DAB Acid. DAB-OH (0.160 g) was added to 1.00 mL of $H_2{}^{18}O$. HCl gas (produced by dripping concentrated H_2SO_4 onto NH_4Cl granules) was bubbled through the solution with stirring until the solid DAB-OH had completely dissolved (approximate pH 0). The solution was heated to 70 °C with stirring. Aliquots (5 μL) were withdrawn intermittently from the reaction mixture, and the progress of the reaction was monitored by following the change in the ν(C=O) band of the Raman spectrum. The DAB-OH was deemed to be fully exchanged to ^{18}O in both of its carboxyl oxygens when the ν(C=O) band had been completely transformed from a narrow (15 cm^{-1} FWHM) single peak at 1709 cm^{-1} to a narrow single peak at 1682 cm^{-1} (approximately 48-h reaction time). The solution was allowed to cool and then adjusted to pH 3 with a small amount of 2 M NaOH, which precipitated the DAB-^{18}OH. The supernatant solution was evaporated off, and the DAB-^{18}OH precipitate was dried and used to make the DAB-^{18}Im, as described below. Besides the 28 cm^{-1} shift of the ν(C=O) band to lower frequency, there were shifts to lower frequency in the 1256 and 797 cm^{-1} bands of 5 and 8 cm^{-1}, respectively.

Synthesis of DAB-Imidazolide. DAB-OH (0.063 g) was dissolved in 5 mL of dry THF, and to this was added 0.095 g of 1,1′-carbonyldiimidazole with stirring at 25 °C. The progress of the reaction was monitored by taking 5-μL aliquots and following the disappearance of the DAB-OH ν(C=O) Raman band at 1709 cm^{-1} and the appearance of the DAB-Im ν(C=O) band at 1691 cm^{-1}. After the reaction had stirred for 3 h, the Raman spectrum indicated complete formation of DAB-Im. The solution was dried, redissolved in 5 mL of $CHCl_3$, and washed two times with 0.5-mL aliquots of 8% bicarbonate solution. The $CHCl_3$ phase was dried to yield 0.066 g of DAB-Im (80.3% yield, slightly yellow solid, mp 109–111 °C). ^1H NMR showed no residual DAB-OH or imidazole. DAB-Im with ^{18}O at the carbonyl oxygen was prepared as described above, except that DAB-^{18}OH was used as the starting material. The shift in the ν(C=O) band was by 27 cm^{-1} from 1691 (^{16}O) to 1664 cm^{-1} (^{18}O). No other Raman bands exhibited a significant ^{18}O isotopic shift.

Preparation of DAB-Acyl-Enzymes. In order to obtain a good quality Raman difference spectrum, we prepared samples of DAB-acyl-enzyme and enzyme alone that were within 5% of each other in concentration. The DAB-acyl-enzyme sample was prepared by adding a 10-fold stoichiometric excess of DAB-Im (3–5 μL, 100 mM in CH_3CN) to a concentrated solution of enzyme (30–50 μL volume, 1–2 mM buffer: 10 mM MES, 5 mM $CaCl_2$, and 100 mM NaCl) at pH 5.5. A "twin" enzyme alone sample was prepared by adding an equal volume of CH_3CN (without DAB-Im) to an equal volume of the concentrated enzyme solution. Both samples were allowed to react for 30 min at 20 °C and then applied to identical gel filtration spin-columns. Spin-columns were prepared by adding 0.5 mL of a slurry of Sephadex G-15 (fine) equilibrated with pH 4.5 H_2O to a 1.0-mL tuberculin syringe with a glass wool plug. The columns were spun for 2 min prior to applying the samples in order to eliminate excess interstitial solution. After application to the columns, the samples were allowed to seep in for 1 min and were then spun for 4 min in a benchtop centrifuge. The filtrate (which is used as the sample for Raman measurements) was collected in 0.5-mL Eppendorf tubes, which fit snugly over the ends of the spin-columns. The filtrate was found to contain no excess DAB-Im substrate. The protein concentration was typically only 70% of the applied concentration. The concentrations of the enzymes were determined spectrophotometrically ($\epsilon_{280}{}^{0.1\%}$ = 1.17; Matsubara *et al.*, 1965). The DAB-acyl-enzymes of WT, N155G, CHT, and TRY were all prepared successfully. As with DAB-CHT (Argade, 1984), formation of DAB-WT, DAB-N155G, and DAB-TRY results in the appearance of a strong UV absorbance band centered near 330 nm.

Three control experiments were carried out to confirm that DAB-WT, like DAB-CHT, forms a 1:1 adduct only at the enzyme's active site. (1) Preincubation of the WT with the irreversible serine protease inhibitor PMSF, followed by reaction with DAB-Im, completely prevented the appearance of the 330-nm band. (2) Formation of the DAB-WT complex completely inhibited the turnover of the peptide substrate *N*-succinyl-Ala-Ala-Pro-Phe-*p*-nitroanilide (s-AAPF-*p*na). (3) Reaction of WT with a range of DAB-Im concentrations

[1] Abbreviations: WT, wild-type subtilisin-BPN′; N155G, Asn155→Gly subtilisin-BPN′; CHT, α-chymotrypsin; TRY, bovine trypsin; DAB-Im, *p*-(dimethylamino)benzoylimidazolide; DAB-OH, *p*-(dimethylamino)-benzoic acid; DAB-OEt, *p*-(dimethylamino)benzoic acid ethyl ester; the DAB- prefix before an enzyme abbreviation (e.g., DAB-CHT) indicates the *p*-(dimethylamino)benzoylacyl-enzyme intermediate of that enzyme; sAAPF-*p*na, *N*-succinyl-Ala-Ala-Pro-Phe-*p*-nitroanilide. All amino acids are in the L configuration unless otherwise specified. Protease substrate residues (P_1, P_2, ...) and their respective binding sites (S_1, S_2, ...) are designated using the nomenclature of Schecter and Berger (1967).

(0–2 stoichiometric equiv) showed that the formation of DAB-WT (as measured by the ratio of absorbances, A_{330}/A_{280}) is maximal with 1 equiv (maximal $A_{330}/A_{280} = 0.8$). Above 1 stoichiometric equiv of DAB-Im, no further acylation is observed.

A_{330}/A_{280} for DAB-N155G was found to be equal to that of DAB-WT, yet whereas the DAB-WT formed completely after 3 min, the N155G required approximately 30 min for complete acylation. DAB-TRY was formed as quickly and completely as DAB-WT upon reaction of DAB-Im and TRY at pH 5.5. It was somewhat surprising that the DAB-acyl-enzyme of TRY could be formed at all, since it prefers smaller charged amino acids at the substrate P_1 position, whereas DAB-Im resembles the large hydrophobic P_1 side chains preferred by CHT and WT.

UV-vis Absorbance and Kinetic Measurements. Absorbance spectra and deacylation rate constants, k_3, for DAB-acyl-enzymes were measured on a Varian DMS 300 spectrophotometer. Typically, 4 μL of the DAB-acyl-enzyme sample (1–2 mM, pH 4.5) was added to 400 μL of buffer (100 mM buffer salt) in a 1.0-cm quartz cuvette and scanned between 250 and 400 nm at 200 nm/min. The λ_{max} was calculated by the spectrophotometer and was found to be precise to ±0.2 nm. The k_3 values were measured using the same sample and monitoring the decrease in $\log(A_{330})$ over a 10-min to 3-h period (depending on the reactivity of the acyl-enzyme). Good linear plots indicative of first-order deacylation kinetics were observed for all of the DAB-acyl-enzymes. k_3 was calculated directly from the slope of the plot of $\log(A_{330})$ versus time, according to the equation, $\log A_{330} = -(k_3/2.303)t$. The buffer salts used in kinetic measurements were acetate (pH 4.0 and 5.4), phosphate (pH 6.3, 7.2, and 7.8), borate (pH 9.3), and carbonate (pH 10.7). Sample temperature in the spectrophotometer was 28 ± 1 °C.

Raman Data Collection. Raman difference spectra of DAB-WT, DAB-N155G, DAB-CHT, and the model compound, DAB-OEt, were collected using the Raman microscope described previously (Patapoff *et al.*, 1988). For these experiments, the system was modified such that the incident radiation was focused directly on a sample capillary on the microscope stage, and the scattered light was collected through the 10× objective at an 85-deg angle. A homemade brass mount on the microscope stage allowed reproducible placement of the sample capillary once the collection optics had been aligned. The brass mount was equipped with a Pelletier cooler, which was used to maintain the sample temperature at 5 °C. The incident radiation used was 200 mW/488.0 nm from a Spectra-Physics Model 171 argon ion laser. A Spex Triplemate spectrograph, with two 300 grates/mm gratings in the filter stage and a 1200 grates/mm grating in the spectrograph stage, was used to disperse the light onto a Tracor-Northern 6500 intensified diode array detector. The TN-6500 detector allowed measurement of Raman intensities across a 1200 cm^{-1} region in a single shot. The spectrograph stage entrance slit was set at 180 μm, resulting in a spectral slit width of 10 cm^{-1}. The spectra were calibrated using a Raman spectrum of indene, and the band positions of the Raman spectra were found to be reproducible to ±1 cm^{-1}.

The Raman spectra of DAB-TRY were obtained on the classical Raman spectrometer, which has a Spex 1301 scanning monochromator and a simple photon counting PMT that requires much longer spectral accumulation times for good quality difference spectra. Consequently, these spectra are noisier than those obtained on the Raman microscope system.

Table 1: Deacylation Rate Constants, k_3, and Absorbance, λ_{max}, for DAB-Acyl-Enzymes and DAB-OEt at pH 7.8[a]

acyl-enzyme	λ_{max} (nm)[b]	k_3 ($\times 10^4$ s^{-1})[b]
DAB-WT	329.6 ± 0.3 (7)	7.6 ± 0.5 (7)
DAB-N155G	327.6 ± 0.5 (8)	0.09 ± 0.01 (9)
DAB-CHT	327.3 ± 0.3 (9)	0.01 ± 0.01 (3)
DAB-TRY	333.7 ± 0.3 (3)	0.61 ± 0.05 (3)
DAB-OEt	315.0 ± 0.2 (2)	0.007 ± 0.001 (2)

[a] Sample preparation and measurement conditions are as described in the Materials and Methods section. [b] Listed λ_{max} and k_3 values are the mean of N separate measurements. N is given in parentheses below each respective value. The given uncertainties are standard deviations from the mean.

The protocol for manipulating the raw Raman data was as follows. The DAB-acyl-enzyme and enzyme spectra were base-lined identically to correct for different fluorescent backgrounds. Both spectra were then normalized such that the spectral intensity was 10.0 at the peak of the 1450 cm^{-1} protein band and 0.0 at 1500 cm^{-1}. The enzyme spectrum was then subtracted from the DAB-acyl-enzyme spectrum until the 1450 cm^{-1} protein band disappeared, resulting in a flat base line between 1400 and 1500 cm^{-1}. Protein bands at 1000 and 1240 cm^{-1} were also monitored to insure correct subtraction. The commercially available program Spectra-Calc (Galactic Industries, Inc.) was found to be especially useful for carrying out the spectral subtractions, as it allows the user to vary the subtraction factor and see the results in real time on the computer screen. Typically, the amount of enzyme alone spectrum needed to completely subtract out the protein contribution from the DAB-acyl-enzyme spectrum ranged between 0.97 and 1.03. For the Raman difference spectra shown in this work, the noise level [as measured by the method of Yue *et al.* (1989)] ranged from 1 to 3% of the total signal of the enzyme's amide I Raman band. Difference spectra signal levels were characterized by a carbonyl stretching band, ν(C=O), whose intensity was 15–20% of the amide I.

RESULTS AND DISCUSSION

Kinetics of DAB-Acyl-Enzyme Deacylation. The usual steady-state kinetic treatment of serine protease catalysis results in the following simplified reaction scheme:

$$E + S \underset{k_{-1}}{\overset{k_1}{\rightleftarrows}} E{\cdot}S \overset{k_2}{\rightleftarrows} E\text{–}P_2 + P_1 \overset{k_3}{\rightleftarrows} E + P_2$$

[for a review, see Walsh (1979)]. Whereas for peptide and amide acylation, k_2 is the rate-limiting step, for ester and imidazolide deacylation, k_3 is rate-limiting. Consequently, the DAB-acyl-enzymes can be trapped at low pH after initial acylation with DAB-Im, and k_3 is easily determined by following the first-order disappearance of the absorbance. Table 1 lists k_3 measured at pH 7.8 for DAB-WT, DAB-N155G, DAB-CHT, and DAB-TRY. The k_3 values are the averages of a number of measurements (shown in parentheses in Table 1) carried out on different DAB-acyl-enzyme sample preparations. The uncertainties are standard deviations from the mean of the separate measurements.

At pH 7.8, DAB-WT has a deacylation rate constant, $k_3 = 7.6 \times 10^{-4}$ s^{-1}; the DAB-N155G deacylation rate is 84-fold slower ($k_3 = 0.09 \times 10^{-4}$ s^{-1}). The loss of transition-state

binding free energy, $\Delta\Delta G^{\ddagger}$, due to a site-directed mutation can be calculated from the kinetic constants, k_{cat} and K_m using the equation, $\Delta\Delta G^{\ddagger} = -RT \ln[(k_{cat}/K_m)^{mut}/(k_{cat}/K_m)^{WT}]$ (Fersht *et al.*, 1985). A different equation must be used to calculate $\Delta\Delta G^{\ddagger}$ for deacylation because k_3 is a first-order rate constant. Since deacylation is an intramolecular base-catalyzed reaction, the effective nucleophile concentrations for DAB-WT and DAB-N155G are equal. Thus, any concentration-dependent terms in the ratio of second-order rate constants are canceled, and the above equation is rewritten as $\Delta\Delta G^{\ddagger} = -RT \ln(k_3^{N155G}/k_3^{WT})$. Using this equation, the N155G $\Delta\Delta G^{\ddagger}$ = 2.6 kcal/mol for DAB-acyl-enzyme deacylation at pH 7.8. For comparison, the N155G $\Delta\Delta G^{\ddagger}$ = 3.3 kcal/mol for the hydrolysis of peptide substrate, sAAPF-*p*na (Carter & Wells, 1990).

Systematic site-directed mutagenesis of tyrosyl-tRNA synthetase has determined that the disruption of a neutral–neutral hydrogen bond results in a loss of binding free energy, $\Delta\Delta G^{\ddagger}$, of between 0.5 and 1.5 kcal/mol, whereas a charged–neutral hydrogen bond disruption costs 3–5 kcal/mol (Fersht *et al.*, 1985). It has been previously noted (Carter & Wells, 1990) that the N155G $\Delta\Delta G^{\ddagger}$ value for sAAPF-*p*na hydrolysis falls into the range for a charged–neutral hydrogen bond, which agrees well with the known structural features (the $N^{\delta 2}$ hydrogen of N155 and the negatively charged transition state). The N155G $\Delta\Delta G^{\ddagger}$ value for DAB-acyl-enzyme deacylation measured here, although 0.7 kcal/mol lower, also suggests a charged–neutral hydrogen bond at the transition state. Its slightly lower $\Delta\Delta G^{\ddagger}$ suggests that the oxyanion hole hydrogen bond does not act as strongly to stabilize the DAB deacylation transition state as it does the sAAPF-*p*na acylation transition state. Although they are often assumed to be equivalent, rigorous acylation and deacylation are not identical elementary processes; thus, to postulate about the structural differences underlying this disparity will demand a great deal more data.

pH Dependence of DAB-Acyl-Enzyme Deacylation Rates. The k_3 values were also measured over a range of pH's from 4 to 10.7. A plot of log k_3 versus pH is shown in Figure 1. All of the DAB-acyl-enzyme deacylation rates show a strong pH dependence. Both DAB-WT and DAB-TRY have strongly sigmoidal plots with an inflection point near pH 7.0. This agrees well with the accepted mechanism of serine protease catalysis in which the catalytic triad histidine (H64 in subtilisin-BPN′) acts as a base to deliver a hydroxide to the acyl-enzyme carbonyl. Protonation of the histidine below pH 7.0 deactivates this base-catalyzed deacylation mechanism. It is presumed that DAB-CHT also follows this mechanism, but because of its extremely slow deacylation rate ($\tau_{1/2}$ = 3–4 days), it was not possible to make a complete plot. The deacylation rates of a variety of other chromophoric acyl-enzymes of CHT have been measured, and all have been found to show a dependence on the pK_a of the active-site histidine near pH 7.2 (Tonge & Carey, 1989).

DAB-N155G shows a sharp rate increase around pH 7.0, yet whereas the DAB-WT and DAB-TRY rates level off between pH 8 and 10, its rate continues to increase such that at pH 10.7 it deacylates only 5.5-fold slower than DAB-WT. It is presumed that the DAB-WT and DAB-TRY rates level off because their histidines are fully deprotonated at approximately pH 9 and cannot further increase their strength as a base. The fact that the DAB-N155G log k_3 continues to increase approximately linearly with pH suggests that, in addition to the natural histidine-catalyzed mechanism, a second deacylation mechanism is at work whose rate is dependent on the concentration of free hydroxide. It has been

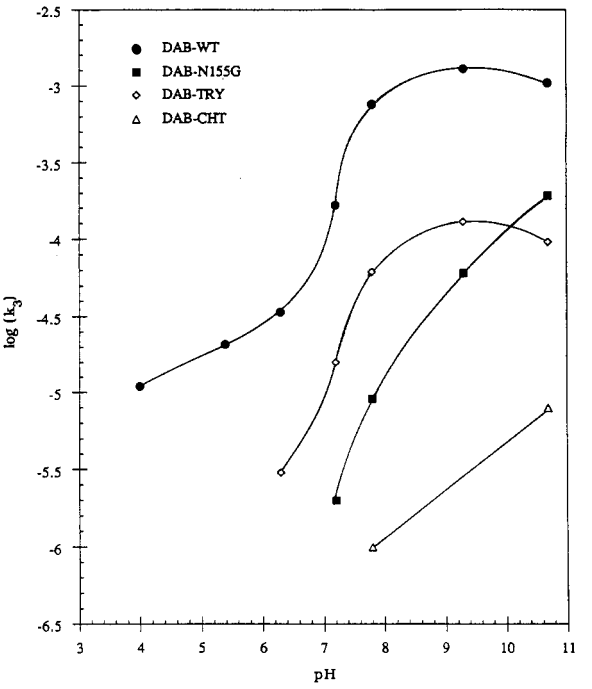

FIGURE 1: Plot of the log of the DAB-acyl-enzyme deacylation rate, k_3, versus pH. The acyl-enzymes are as follows: DAB-WT (●); DAB-N155G (■); DAB-TRY (◇); and DAB-CHT (△). Reaction conditions and buffers used are described in Materials and Methods.

shown that the calculated solvent-accessible van der Waals surface of the carbonyl carbon of a *p*-nitroanilide model substrate increases significantly upon going from the WT to the N155G subtilisin-BPN′ active site (Carter & Wells, 1990). It is reasonable to assume that this greater solvent-accessible surface also exists in DAB-N155G relative to DAB-WT and that it allows free hydroxide nucleophiles to attack from the opposite face of the carbonyl. This competing deacylation mechanism would exist predominantly at higher pH and thus account for the observed pH dependence of DAB-N155G deacylation.

UV-vis Absorbance of DAB-Acyl-Enzymes and the Red Shift. λ_{max} values of the various DAB-acyl-enzymes at pH 7.8 are shown in Table 1. It has been found previously that the absorbance λ_{max} of chromophoric acyl-enzymes of native α-chymotrypsin and subtilisin are greatly red-shifted relative to the denatured acyl-enzymes and model *O*-acylserine peptides in various solvents (Bernhard *et al.*, 1965; Noller & Bernhard, 1965). A typical red shift of approximately 15 nm is observed for all of the DAB-acyl-enzymes studied in this work. DAB-OEt, which has been used in this work as a model compound, has an absorbance λ_{max} at 315.0 nm in aqueous solution, a 14.6-nm shorter wavelength than the DAB-WT λ_{max} (329.6 nm). Interestingly, the λ_{max} of DAB-N155G (327.6 nm) is shifted 2.0 nm to shorter wavelength relative to DAB-WT (i.e., DAB-N155G exhibits 2.0 nm less red shift than DAB-WT). DAB-CHT (327.3 nm) is also less red-shifted than DAB-WT, whereas DAB-TRY has a significantly greater red shift (333.7 nm). DAB-CHT, which has the lowest k_3, also has the lowest λ_{max}. Unfortunately, this relationship does not hold for DAB-TRY which, although it has the most red-shifted λ_{max}, has a lower k_3 than DAB-WT. The λ_{max} values were also measured over a range of pH's, but above pH 7.8 accurate values for DAB-WT were difficult to obtain due to rapid deacylation. The λ_{max} of DAB-CHT was found to shift from 330.3 nm at pH 6.3 to 327.3 nm at pH 7.8. The λ_{max} of DAB-TRY also showed a shift with pH (from 334.7 nm

Chart 1

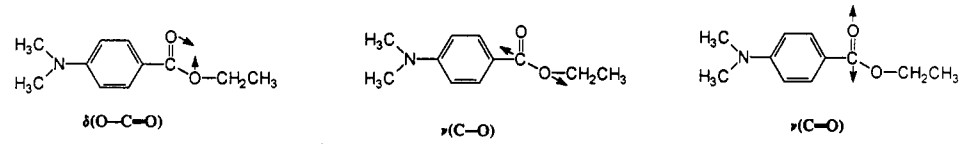

at pH 6.3 to 333.7 nm at pH 7.8 and then to 331.1 nm at pH 9.3), but it was not as clearly correlated with the histidine pK_a near 7.3. Neither DAB-WT nor DAB-N155G showed a shift in λ_{max} with pH between 4 and 7.8. These results indicate that the protonation of the histidine at the CHT and TRY active sites has a much greater effect on the DAB-acyl-enzyme electronic structure than in WT or N155G.

The cause of the red shift and the question of whether it has catalytic significance has been the subject of much study (Bernhard & Lau, 1971; Bernhard & Malhotra, 1974; Argade *et al.*, 1984; Tonge & Carey, 1988). Somehow the native active site brings about either the destabilization of the electronic ground state (LUMO) or the stabilization of the excited state (HOMO). Previously, three mechanisms have been proposed to account for the red shift: (1) an out-of-plane torsion of the acyl-enzyme ester linkage (ground-state distortion) created by active-site forces (Bernhard & Lau, 1971); (2) strong hydrogen bonding to the carbonyl oxygen of the acyl-enzyme (Bernhard & Lau, 1971); and (3) stabilization of the acyl-enzyme electronic excited state by the electrostatic field of the active site (Warshel & Russell, 1984). The results of this work do not rule out any of these three mechanisms, but the finding reported here, that the red shift is decreased by 2.0 nm in DAB-N155G, clearly indicates that the N155 residue of the oxyanion hole is somehow involved. While this would seem to point to mechanism 2, it could be that the three mechanisms are not completely independent. For example, the hydrogen bond formed between N155 and the DAB-WT carbonyl oxygen (mechanism 2) could distort the ester linkage out of the plane (mechanism 1), and the dipole created by the N155 $N^{\delta 2}$ hydrogen, which stabilizes the negatively charged oxyanion, should also stabilize the electronic excited state of the DAB-acyl-enzyme (mechanism 3), which is known be highly charge-separated (Rettig *et al.*, 1979).

Analysis of DAB-Acyl-Enzyme Raman Difference Spectra. Good quality Raman difference spectra were obtained for all four DAB-acyl-enzymes. In order to help with the assignment and analysis of the DAB-acyl-enzyme spectra, Raman spectra of the model ester compound, DAB-OEt, were also measured in a variety of solvents. Of the 11–13 observed Raman bands, seven can be assigned to delocalized motions of the *p*-(dimethylamino)benzoyl moiety (Forster & Hester, 1981). None of these seven bands changes more than 7 cm^{-1} in frequency or 5% in intensity over the range of enzyme active sites (or range of solvents from ether to H_2O for DAB-OEt). At this point it should be noted that the number, intensity, and frequency of the Raman bands in the spectra of all of the DAB-acyl-enzymes clearly indicate the formation of a serine ester and not an imidazolide, as would be expected if a covalent interaction were formed to the active-site histidine. The Raman spectrum of DAB-Im, which is a good model of a DAB–histidine adduct, is markedly different in the 600–1400 cm^{-1} region (data not shown). Another general comment about the spectra that can be made here is that they show no evidence of a quininoid structure, which donor aromatic acceptor type molecules such as DAB are known to adopt (Forster & Hester, 1981). DAB aldehyde, when bound to Zn^{2+}, is characterized by large changes in the frequency and intensity of several Raman bands, which are attributed to the quininoid structure (Callender *et al.*, 1988). None of these quininoid marker bands are visible in any of the DAB-acyl-enzyme difference spectra.

Table 2: Observed Frequencies[a] of Carbonyl-Associated Raman Bands[g] in DAB Compounds

compound, pH/solvent	ν(C═O) (cm^{-1})		ν(C—O) (cm^{-1})		δ(O—C═O) (cm^{-1})	
	^{16}O[b]	^{18}O[c]	^{16}O[b]	^{18}O[c]	^{16}O[b]	^{18}O[c]
DAB-WT						
pH 5	1675	1648	1280	1279	862	853
pH 8.6	1661	1641	1283	1283	862	856
					817	808
DAB-N155G						
pH 5	1692	1660	1282	1280	862	853
pH 8.6	1693	1662	1284	1279	862	854
DAB-CHT						
pH 5	1695	1665	1274	1272	809	801
pH 8.6[d]	1692	nd[f]	1277	nd	817	nd
DAB-TRY						
pH 5	1661	1651	1286	1284	845	843
					808	803
DAB-OEt						
CCl	1705	nd	1279	nd	850	nd
CH_3CN	1696	nd	1281	nd	848	nd
formamide	1676	nd	1285	nd	854	nd
H_2O	1669	nd	1294	nd	856	nd
DAB-OCH_3[e]						
CH_3CN	1706	nd	1292	nd	826	nd
DAB-OH[d]						
THF	1709	1682	1256	1251	797	789
DAB-Im[d]						
THF	1691	1664				

[a] Frequencies are certain to ±1 cm^{-1}. [b] Observed frequency of Raman band in compound with ^{16}O-labeled carbonyl oxygen. [c] Observed frequency of Raman band in compound with ^{18}O-labeled carbonyl oxygen. [d] From this work, data not shown. [e] Data from Argade *et al.*, 1984. [f] nd, not determined. [g] Assignments were made on the basis of published normal mode analyses of DAB-OEt (Forster & Hester, 1981) and methyl and ethyl benzoate (Green & Harrison, 1977) and the ^{18}O shifts observed in this work.

The Raman bands that show the greatest variability among the acyl-enzymes (as well as in the DAB-OEt spectra in various solvents) are the three most strongly associated with the acyl linkage: the carbonyl stretch (ν(C═O)), the ester stretch (ν(C—O)), and the in-plane carboxyl deformation (δ(O—C═O)). A schematic diagram of the coordinates of these vibrational modes is shown in Chart 1 [Note: The size and direction of the arrows in this diagram are approximate and not based on an actual normal mode calculation]. Fortunately, it is also these three bands that are the most interesting in terms of the enzyme mechanism. A listing of the frequencies for these acyl-linkage-associated vibrations in DAB model compounds and the acyl-enzymes is presented in Table 2. The stretching of the carbonyl (ν(C═O)), which leads directly to the formation of the deacylation transition state and would be most directly affected by the oxyanion hole, will be the focus of much of the rest of this discussion.

Raman difference spectra of DAB-WT at pH 5 are shown in Figure 2. The top spectrum (A) in the figure is the DAB-acyl-enzyme difference spectrum with ^{16}O (natural abundance) at the carbonyl oxygen, the middle spectrum (B) is the

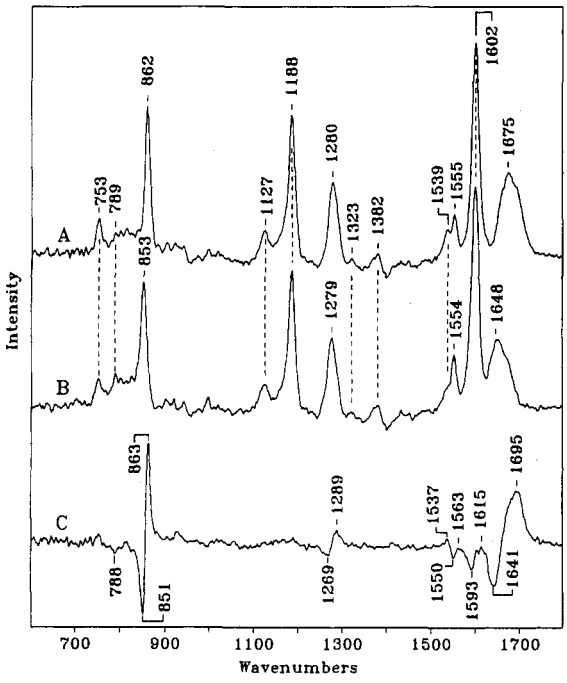

FIGURE 2: DAB-WT (pH 5.0) Raman difference spectra: (A) C=^{16}O-labeled DAB-WT; (B) C=^{18}O-labeled DAB-WT; (C) spectrum B subtracted from spectrum A. Sample preparation and data collection are as described under Materials and Methods.

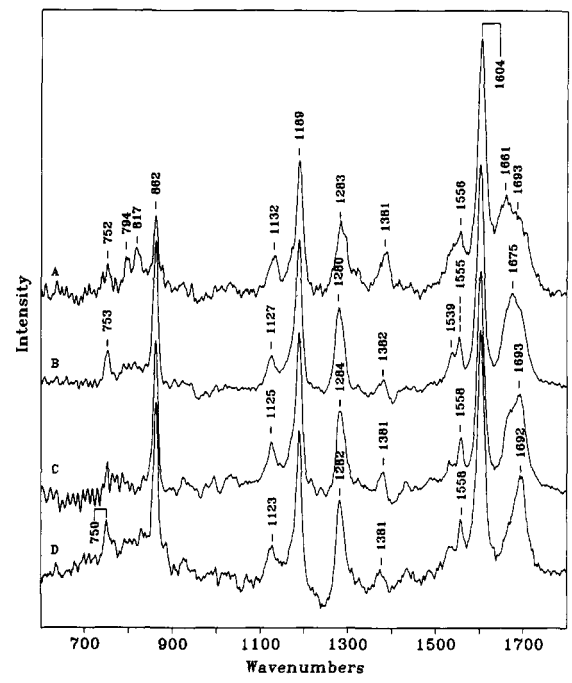

FIGURE 3: Comparison of DAB-WT and DAB-N155G Raman difference spectra: (A) pH 8.6, DAB-WT; (B) pH 5.0, DAB-WT; (C) pH 8.6, DAB-N155G; (D) pH 5.0, DAB-N155G. Sample preparation and data collection are as described under Materials and Methods.

^{18}O-labeled difference spectrum, and the bottom spectrum (C) is the residual of the ^{18}O spectrum subtracted from the ^{16}O spectrum. This ^{16}O – ^{18}O residual (C) shows more clearly which Raman bands shift upon isotopic substitution of the carbonyl oxygen. A previous study of the FT-IR difference spectra of acyl-chymotrypsins (Tonge *et al.*, 1991) has shown that artifactual ν(C=O) intensity can appear in the 1660–1700 cm^{-1} region due to changes in the enzyme amide I vibrational mode of the acyl-enzyme. In order to establish that the DAB-WT ν(C=O) bands measured in this work contain no artifactual intensity, difference spectra of ^{18}O-labeled DAB-acyl-enzymes were measured. Because only the carbonyl of the DAB moiety is ^{18}O-labeled, any Raman intensity in the 1650–1710 cm^{-1} range that undergoes an isotopic shift can be assigned unambiguously to the DAB-acyl-enzyme ν(C=O). The Raman difference spectrum of ^{18}O-labeled pH 5.0 DAB-WT (Figure 2B) confirms that the broad band with a peak at 1675 cm^{-1} is due to the ν(C=O). There is a 27 cm^{-1} shift to lower frequency (1675→1648 cm^{-1}), and more importantly, the whole band shifts without any splitting or change in shape. Similar quality ^{16}O and ^{18}O difference spectra were obtained for all of the DAB-acyl-enzymes and confirm in each case that the intensity in the 1650–1700 cm^{-1} region is due solely to the ν(C=O).

Comparison of DAB-WT and DAB-N155G ν(C=O) Bands. The ν(C=O) of DAB-WT at pH 5.0 is broader (55 cm^{-1} FWHM) and less symmetric than that of the model compound DAB-OEt in H_2O. The band shape suggests at least two underlying component bands: one at 1675 cm^{-1} and the other near 1695 cm^{-1}. On the basis of the relative frequencies of DAB-OEt in various solvents (see Table 2), it is possible to make a qualitative description of the solvent environments experienced by these two ν(C=O) components: the 1695 cm^{-1} frequency corresponds to a carbonyl oxygen in an environment resembling acetonitrile, while the 1675 cm^{-1} resembles a formamide solvent environment. Apparently, a range of interactions is available to the DAB-WT acyl-enzyme carbonyl, and it partitions into at least two populations, which experience quite different active-site environments. The frequency and band shape of the ν(C=O) of DAB-N155G at pH 5.0 (see Figure 3D) significantly differs from those of DAB-WT. The DAB-N155G ν(C=O) is narrower (47 cm^{-1} FWHM) and consists primarily of a single strong component with a well-defined peak at 1693 cm^{-1}. There is almost no intensity in the 1675 cm^{-1} region that is more prominent in DAB-WT. Clearly, on the basis of its absence from the DAB-N155G difference spectrum, as well as the qualitative correlation to formamide solvent, the 1675 cm^{-1} component of the DAB-WT ν(C=O) can be assigned confidently to a carbonyl with its oxygen hydrogen-bonded to the N155 residue of the oxyanion hole. This assignment is supported by the previously reported resonance Raman spectra of the [(5-methyl-2-thienyl)acryloyl]-acyl-enzymes of WT and N155L subtilisin-BPN′ (hereafter, 5MeTA-WT and 5MeTA-N155L) at pH 9.8 (Tonge & Carey, 1990b), which bear a great deal of similarity to the DAB-acyl-enzymes. Like DAB-WT, 5MeTA-WT has a broad ν(C=O) band that consists of two components with peaks at 1673 and 1695 cm^{-1}, whereas 5MeTA-N155L has a substantially narrower ν(C=O) that consists of a single peak at 1705 cm^{-1}. As with the 1675 cm^{-1} component of the DAB-WT ν(C=O), the lower frequency 1673 cm^{-1} component of 5MeTA-WT is assigned to a population of carbonyls in which the oxygen is forming strong hydrogen bonds with the oxyanion hole.

There is one notable difference between 5MeTA-WT and DAB-WT. At pH 5.0 the ν(C=O) of 5MeTA-WT consists of a single band at 1703 cm^{-1} (Tonge & Carey, 1990a); its oxyanion hole bound population at 1673 cm^{-1} appears only upon titration of the active-site histidine above pH 7. In contrast, even at pH 5.0, DAB-WT has a large population of strongly oxyanion hole bound carbonyls at 1675 cm^{-1}. Presumably, at pH 5.0, this population cannot undergo hydrolysis because the protonated histidine cannot act as a base and deliver the nucleophile. Thus, the deprotonation of the histidine N$^{\epsilon 2}$ is not essential to the formation of the

hydrogen bonds between the DAB-WT acyl-enzyme and the oxyanion hole, but as will be discussed in the section on pH dependence, the histidine does act to strengthen the interaction. Finally, it should be noted that, although their ν(C=O) bands differ drastically, all of the other DAB-WT and DAB-N155G vibrational modes are virtually identical in frequency and intensity. The lack of any significant changes in these other modes suggests that the effect of the N155G mutation is indeed localized to the oxyanion hole region of the active-site which in turn only affects the carbonyl bond of the DAB-acyl-enzyme.

pH Dependence of DAB-WT and DAB-N155G Raman Difference Spectra. As discussed previously, the deacylation rates of DAB-acyl-enzymes are dependent on the pK_a of the active-site histidine. Above pH 7.3, the $N^{\epsilon 2}$ of the histidine is in its deprotonated form and can act as a base to deliver a hydroxide to the electrophilic center of the acyl-enzyme carbonyl. As shown in Figure 1, at pH 8.6 the rate of DAB-WT deacylation is approximately 100-fold greater than that at pH 5.0. Figure 3A shows the pH 8.6 DAB-WT (^{16}O at the carbonyl oxygen) difference spectrum, taken at 5 °C, between 0 and 50 min after the adjustment to pH 8.6. Although deacylation is occurring, comparison of spectra taken at t = 5–10 min to those taken at t = 45–50 min shows no significant differences, indicating that product build-up is still slow on the time scale of the Raman measurement. There is a strong Raman band in the 1380–90 cm^{-1} region due to the symmetric carboxylate stretch of the product molecule, deprotonated DAB-OH. Raman difference spectra taken of DAB-WT after 24 h at pH 8.6 and 20 °C show that this 1380–90 cm^{-1} band increases until its intensity is comparable to that of the 1604 cm^{-1} band. Concomitant with this product build-up over 24 h, the ν(C=O) intensity between 1640 and 1700 cm^{-1} disappears completely, which further supports the assignment of the intensity in this region to the DAB-WT acyl-enzyme ν(C=O) and not to the enzyme amide I or the ν(C=O) of the bound product, DAB-OH.

The ν(C=O) of DAB-WT at pH 8.6 (see Figure 3A) is considerably broader (73 cm^{-1} FWHM) than at pH 5.0 (see Figure 3B); the peak of the lower frequency oxyanion hole bound population has shifted from 1675 (at pH 5.0) to 1661 cm^{-1}. Apparently, the hydrogen-bonding interaction between the DAB-WT carbonyl and the oxyanion hole that exists at pH 5.0 increases in strength at pH 8.6, resulting in the observed 14 cm^{-1} shift in ν(C=O). Similar pH-induced ν(C=O) shifts of 30 and 15 cm^{-1} have been observed in the resonance Raman spectra of 5MeTA-WT and 5-MeTA-CHT, respectively (Tonge & Carey, 1989, 1990a). In terms of the qualitative relationship between the ν(C=O) frequency and the solvent environment, the carbonyl of DAB-WT at pH 8.6 (1661 cm^{-1}) is experiencing stronger hydrogen-bonding interactions than the carbonyl of DAB-OEt in H_2O (1668 cm^{-1}). Similarly, the ν(C=O) bands of 5MeTA-WT and 5MeTA-CHT at pH 9.8 are, respectively, 13 and 5 cm^{-1} lower in frequency than the ν(C=O) of the model compound, 5MeTA methyl ester in H_2O solvent (Tonge & Carey, 1989). Apparently, the oxyanion hole has a stronger electron-withdrawing effect on the carbonyl than the hydrogen bonds of bulk H_2O. As mentioned previously, the serine protease active site has been proposed to contain a unique electrostatic field that brings about the large red shifts in the absorbance of the chromophoric acyl-enzymes relative to their model esters in H_2O (Tonge & Carey, 1988; Warshel & Russell, 1984). It is reasonable to presume that these same electrostatic forces could also cause the anomalously low ν(C=O) values described above.

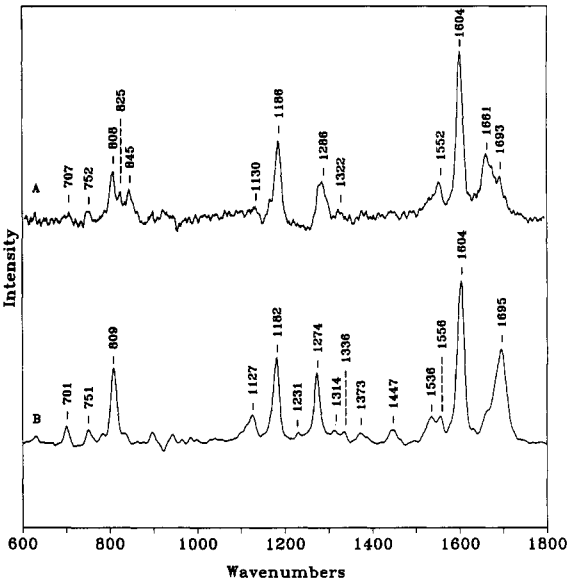

FIGURE 4: DAB-TRY and DAB-CHT Raman difference spectra: (A) pH 5.0, DAB-TRY; (B) pH 5.0, DAB-CHT. Sample preparation and data collection are as described under Materials and Methods.

In contrast to DAB-WT, there is no evidence of DAB-OH product in the pH 8.6 DAB-N155G difference spectra shown in Figure 3C. Indeed, even after 72 h, stored at 3 °C (pH 8.6) there is no significant deacylation of DAB-N155G due to its much slower rate of deacylation. There is no significant shift in the frequency of the DAB-N155G ν(C=O) band at pH 8.6 relative to its pH 5.0 spectrum (Figure 3D). There is some increase in ν(C=O) intensity in the 1670 cm^{-1} region and a 5 cm^{-1} broadening (52 cm^{-1} FWHM) at the higher pH. Although DAB-N155G does lack one oxyanion hole hydrogen-bond donor (N155), this slight increase in the lower frequency shoulder of its ν(C=O) could indicate that its carbonyl oxygen is able to form a hydrogen bond with the remaining S221 backbone amide hydrogen at the higher pH.

Comparison of DAB-TRY and DAB-CHT Raman Difference Spectra. The Raman difference spectrum of DAB-TRY at pH 5.0 is shown in Figure 4A. As in DAB-WT, the ν(C=O) band is broad and appears to consist of two component bands: a higher frequency component that peaks at 1693 cm^{-1} and a lower frequency component that peaks at 1661 cm^{-1}. Surprisingly, the frequency of this latter component is the same as that of the oxyanion hole bound population in DAB-WT at pH 8.6 (and 14 cm^{-1} lower than that of DAB-WT at pH 5.0). Apparently, even at pH 5.0, DAB-TRY forms hydrogen-bonding interactions with the oxyanion hole that are comparable to those of DAB-WT at pH 8.6.

The pH 5.0 DAB-CHT difference spectrum is shown in Figure 4B. Both the pH 5.0 and 8.6 (not shown) DAB-CHT spectra closely resemble the previously published pH 7.0 DAB-CHT Raman difference spectrum (Argade *et al.*, 1984). The ν(C=O) band is narrow (35 cm^{-1} FWHM),, with a single peak at 1694 cm^{-1} that more closely resembles the ν(C=O) of DAB-N155G than that of DAB-WT. In fact, it is 12 cm^{-1} narrower than the N155G ν(C=O), with virtually no intensity in the 1675 cm^{-1} region to suggest any hydrogen-bonding interaction with the oxyanion hole. Moreover, at pH 8.6, ν(C=O) exhibits no shift to lower frequency and only the appearance of a very weak shoulder on the lower frequency side.

Clearly, the Raman data show us that DAB-TRY can make strong oxyanion hole hydrogen bonds, whereas DAB-CHT appears to be poorer than even the DAB-N155G mutant at

forming these bonds. This difference is reflected in the substantially greater deacylation rate of DAB-TRY versus DAB-CHT. It is surprising that DAB-CHT is such a poor acyl-enzyme. DAB-CHT would be expected to be faster than DAB-TRY on the basis of its well-characterized preference for peptide substrates with large hydrophobic side chains at the P_1 position. It appears that these simpler acyl-enzymes do not obey the same binding determinants as the better peptide substrates. It had been found that, depending on the chromophore, CHT could be either 20-fold faster or slower than the corresponding WT subtilisin acyl-enzyme. The (4-amino-3-nitrocinnamoyl)-CHT deacylates 22 times faster than the corresponding WT acyl-enzyme, whereas 5-MeTA-CHT is 4 times slower than 5-MeTA-WT (Tonge & Carey, 1990). While the Raman data unambiguously show that the oxyanion hole can occur in the faster DAB-WT and DAB-TRY, it does not shed much light on the possible structural factors that prevent the DAB-CHT from also forming this interaction. One intriguing piece of evidence that the DAB-CHT structure is highly perturbed is the anomalously low frequency of its δ(O—C=O) band (52 cm^{-1} lower than in DAB-WT). Although this band has not been mentioned in any previous Raman studies of the acyl-enzymes, its association with the scissile acyl linkage has been confirmed here by the ^{18}O-labeled spectra. Unfortunately, the correlation of the frequency of the δ(O—C=O) band with structural changes is not clear-cut. Large frequency changes are observed for changes in the DAB model compound ester substituent (see Table 2), but this is difficult to relate to the acyl-enzymes, which are all serine esters. A further complication is found in the pH 5.0 DAB-TRY and pH 8.6 DAB-WT difference spectra, which both show a similar splitting pattern in their δ(O—C=O) bands. Further investigations of this vibrational mode are planned.

Correlation of Acyl-Enzyme Raman Difference Spectra with Crystal Structures. Of great interest toward interpreting the DAB-TRY and WT Raman spectra is the recently solved crystal structure of the acyl-enzyme guanidinobenzoyl-TRY, at pH 5.0 (Mangel *et al.*, 1990), as well as a time-resolved Laue study at pH 8.5 (Singer *et al.*, 1993). The guanidinobenzoyl moiety is structurally very similar to DAB and deacylates with a very similar rate (0.16×10^{-4} s^{-1}, at pH 7.4, 25 °C; Mangel *et al.*, 1990). Both of the crystal structures show that the acyl-enzyme carbonyl carbon center is, in fact, distorted tetrahedrally with a lengthened carbonyl bond length. The tetrahedral distortion brings the carbonyl oxygen nearer to the oxyanion hole with O–N contact distances (3.2 and 3.3 Å), indicating the formation of weak hydrogen bonds (Mangel *et al.*, 1990). The carbonyl bond length at pH 5.0 is 1.24 Å, which is substantially longer than the prototypical benzoyl ester carbonyl bond length of 1.18 Å (Mangel *et al.*, 1990). On the basis of its structural and functional similarity, it is reasonable to assume that DAB-TRY at pH 5.0 has a similar tetrahedrally distorted carbonyl carbon center. Furthermore, the great similarity of the pH 5.0 DAB-TRY and the pH 8.6 DAB-WT ν(C=O) bands allows us to propose that the pH 8.6 DAB-WT structure also closely resembles the pH 5.0 guanidinobenzoyl-TRY crystal structure: a tetrahedrally distorted carbonyl carbon center. Normally, such a distorted structure would be expected to exist only transiently along the reaction coordinate for the base-catalyzed hydrolysis of an ester in aqueous solution. Apparently, the specific transition-state-stabilizing forces at the enzyme active site (such as the oxyanion hole) allow these distorted structures to exist in the stable ground-state forms of the DAB-WT and DAB-TRY acyl-enzymes.

As for CHT, the crystal structures of two photoreversible cinnamoyl-CHT acyl-enzymes (Stoddard *et al.*, 1990), as well as the older structure of indolylacryloyl-CHT (Henderson, 1970), both show completely planar sp^2 carbonyl centers. If we assume that a similarly planar carbonyl exists in DAB-CHT (which Raman spectroscopy shows does not interact strongly with the oxyanion hole), it is reasonable to make the general hypothesis that a certain amount of distortion necessarily accompanies the formation of good oxyanion hole hydrogen bonds—although the cause-and-effect relationship remains unclear.

Correlation of ν(C=O) to Carbonyl Bond Lengthening and Deacylation Rate Constants. The force constant of a molecular vibration depends on the internuclear distance, among other factors. A strong empirical linear relationship has been found to exist between the ν(C=O) frequencies (from IR data) and the carbonyl bond lengths, r(C=O) (from crystallographic data) (Horvath *et al.*, 1987). This relationship has been used previously to estimate r(C=O) values from resonance Raman ν(C=O) data of acyl-enzymes (Tonge & Carey, 1990b). Using the Raman ν(C=O) data from Table 2 of this work, the r(C=O) of DAB-WT is 1.230 Å at pH 5.0 and 1.237 Å at pH 8.6—a 0.007-Å lengthening. The r(C=O) of DAB-N155G is 1.222 Å at both pH 5.0 and 8.6, which is 0.015 Å shorter than the carbonyl bond in the most active form of DAB-WT. The calculated r(C=O) shortening of 5-MeTA-N155L versus 5-MeTA-WT is an identical 0.015 Å (Tonge & Carey, 1990b). The pH 5.0 DAB-TRY r(C=O) is 1.237 Å, which agrees well with the observed 1.24-Å r(C=O) from the crystal structure of guanidinobenzoyl-TRY at pH 5.0 (Mangel *et al.*, 1990).

It has also been shown that a linear correlation exists between the deacylation rate and the ν(C=O) frequency for a number of acyl-enzymes of WT and CHT (Tonge & Carey, 1990b). This correlation suggests that the strength of the hydrogen bond between the acyl-enzyme carbonyl and the oxyanion hole is the primary determinant of the deacylation rate. Furthermore, the relationship between ν(C=O) and r(C=O) allows deacylation rates to be correlated with the lengthening of the acyl-enzyme carbonyl bond. Hence, it was concluded that a 0.015-Å increase in r(C=O) corresponds to a 500-fold increase in rate (Tonge & Carey, 1990b). More recently, using ν(C=O) frequencies and newly measured deacylation rates of the *cis* conformers of 5-MeTA-CHT and TA-CHT, the correlation has been extended to cover a 16 300-fold range of deacylation rates (Tonge & Carey, 1992). Using the pH 8.6 DAB-acyl-enzyme Raman (Table 2) and kinetic data (Table 1) from this work, a similar plot has been created and is shown in Figure 5, together with the data of Tonge and Carey (1990b).

Interestingly, although the three DAB-acyl-enzyme points do not fall on the same line as the acyl-enzyme data of Tonge and Carey, they do form a parallel line below it. Why do the DAB-acyl-enzymes fail to fit the line of Tonge and Carey? All of the acyl-enzymes used by Tonge and Carey are α,β-unsaturated arylacryloyl, with deacylation rates on the order of 100-fold higher than the DAB-acyl-enzymes. The increased activity of the arylacryloyl-acyl-enzymes does not result completely from the electronic structure of this type of substituent. The base-catalyzed hydrolysis rate, k_{OH^-}, of the imidazolide 5-MeTA-Im (0.013 s^{-1}, pH 10.4; Tonge & Carey, 1989) is only 3-fold greater than that of DAB-Im (0.0045 s^{-1}, pH 10.4; this work). Consequently, it must be concluded that

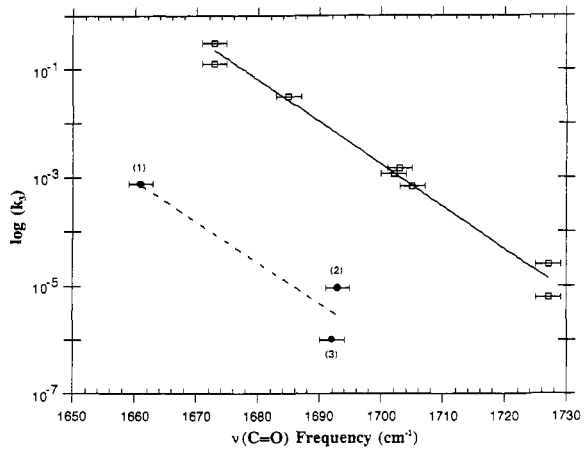

FIGURE 5: Plot of log k_3 versus ν(C=O) at pH 8.6. The □ and solid line represent α,β-unsaturated arylacryloyl-acyl-enzyme data and the linear regression fit from Tonge and Carey (1992). The ●'s represent the pH 8.6 (1) DAB-WT, (2) DAB-N155G, and (3) DAB-CHT data of this work, and the dashed line is the linear regression fit to these data points (R = 0.936).

the faster deacylation rates of the α,β-unsaturated arylacryloyl-acyl-enzymes are due primarily to more favorable enzyme-binding contacts, most likely with the enzyme's S_1 binding site. Apparently, the oxyanion hole binding interaction is not a significant factor in the 100-fold difference in rates. The fact that the DAB-acyl-enzyme line in Figure 5 is parallel with that observed for the acyl-enzymes of Tonge and Carey indicates that the oxyanion hole is functioning with an equivalent efficiency: rates increase as the hydrogen-bonding increases (ν(C=O) decreases). Indeed, it can be argued on the basis of its substantially lower ν(C=O) frequency at pH 8.6 (1661 versus 1673 cm^{-1}) that the oxyanion hole is functioning even better in DAB-WT than in 5-MeTA-WT. Possibly, the inability of the DAB moiety to make the more distal binding interactions allows its carbonyl to move nearer to the oxyanion hole. Consequently, the gain in the oxyanion hole interaction is nullified by improper positioning for another step of the deacylation mechanism (e.g., productive nucleophilic attack), resulting in a slower rate. Regardless, the oxyanion hole is functioning in the deacylation of the DAB-acyl-enzymes in a manner consistent with that observed previously (Tonge & Carey, 1990b).

SUMMARY

Raman difference spectroscopy has been used to measure the hydrogen-bonding interaction between the scissile carbonyl oxygen and the oxyanion hole in the chromophoric DAB-acyl-enzymes of wild-type and N155G subtilisin-BPN′, α-chymotrypsin, and bovine trypsin. Strong oxyanion hole hydrogen bonding exists in DAB-WT (even at inactive pH), although modeling studies have predicted that these bonds cannot form due to the planarity of the carbonyl (Matthews *et al.*, 1975). Surprisingly, DAB-TRY also forms strong oxyanion hole hydrogen bonds, but DAB-CHT appears to be able to make only a very weak interaction. As with previously studied acyl-enzymes (Tonge & Carey, 1990), a strong linear correlation exists between the oxyanion hole hydrogen bonding (as measured by the ν(C=O) frequency) and the deacylation rate. On the basis of their structural and functional similarity to guanidinobenzoyl-TRY, we have postulated that a tetrahedrally distorted carbonyl exists in both DAB-TRY and DAB-WT (as it does in the guanidinobenzoyl-TRY crystal structure) and that this distortion is essential for strong oxyanion hole hydrogen bonding.

ACKNOWLEDGMENT

We are grateful to Dr. James Wells and Dr. Paul Carter of Genentech, Inc., for the gift of N155G subtilisin-BPN′.

REFERENCES

Argade, P. V., Gerke, G. K., Weber, J. P., & Peticolas, W. L. (1984) *Biochemistry 23*, 299–304.
Bender, M. L. (1962) *J. Am. Chem. Soc. 84*, 2582.
Bernhard, S. A., & Lau, S. J. (1971) *Cold Spring Harbor Symp. Quant. Biol. 36*, 75–83.
Bernhard, S. A., & Malhotra, O. P. (1974) *Isr. J. Chem. 12*, 471–481.
Bernhard, S. A., Lau, S. J., & Noller, H. (1965) *Biochemistry 4*, 1108–1118.
Brady, L., Brzozowski, A. M., Derewenda, Z. S., Dodson, E., Dodson, G., Tolley, S., Turkenburg, J. P., Christiansen, L., Huge-Jensen, B., Norskov, L., Thim, L., & Menge, U. (1990) *Nature 343*, 767–770.
Bryan, P., Pantoliano, W., Quill, S. G., Hsiao, H.-Y., & Poulos, T. (1986) *Proc. Natl. Acad. Sci. U.S.A. 83*, 3742–3745.
Callender, R., Chen, D., Lugtenburg, J., Martin, C., Rhee, K. W., Sloan, D., Vandersteen, R., & Yue, K. T. (1988) *Biochemistry 27*, 3672–3681.
Carter, P., & Wells, J. A. (1988) *Nature 332*, 564–568.
Carter, P., & Wells, J. A. (1990) *Proteins: Struct., Funct., Genet. 7*, 335–342.
Carter, P., Bedouelle, H., & Winter, G. (1985) *Nucleic Acids Res. 13*, 4431–4443.
DelMar, E. G., Largman, C., Brodrick, J. W., & Geokas, M. C. (1979) *Anal. Biochem. 99*, 316–320.
Fersht, A. R., Shi, J. P., Knill-Jones, J., Lowe, D. M., Wilkinson, A. J., Blow, D. M., Brick, P., Carter, P., Waye, M. M. Y., & Winter, G. (1985) *Nature 314*, 235–238.
Forster, M., & Hester, R. E. (1981) *J. Chem. Soc., Faraday Trans. 2 77*, 1535–1545.
Green, J. H. S., & Harrison, D. J. (1977) *Spectrochim. Acta 33A*, 583–587.
Hartley, B. S. (1970) *Philos. Trans. R. Soc. London B 257*, 77–87.
Henderson, R. (1970) *J. Mol. Biol. 54*, 341–354.
Horvath, G., Illenyi, J., Pusztay, L., & Simon, K. (1987) *Acta Chim. Hung. 124*, 819–822.
Kossiakoff, A. A. (1987) in *Biological Macromolecules and Assemblies Volume 3: Active Sites of Enzymes* (Jurnak, F. A., & McPherson, A., Eds.) pp 369-412, Wiley & Sons, New York.
Kraut, J. (1977) *Annu. Rev. Biochem. 46*, 331–358.
Liao, D.-I., Breddam, K., Sweet, R. M., Bullock, T., & Remington, S. J. (1992) *Biochemistry 31*, 9796–9812.
MacClement, B. A. E., Carriere, R. G., Phelps, D. J., & Carey, P. R. (1981) *Biochemistry 20*, 3438–3447.
Mangel, W. F., Singer, P. T., Cyr, D. M., Umland, T. C., Toledo, D. L., Stroud, R. M., Pflugrath, J. W., & Sweet, R. M. (1990) *Biochemistry 29*, 8351–8357.
Matsubara, H., Kasper, C. B., Brown, D. M., & Smith, E. L. (1965) *J. Biol. Chem. 240*, 1125–1130.
Matthews, D. A., Alden, A. A., Birktoft, J. J., Freer, S. T., & Kraut, J. (1975) *J. Biol. Chem. 250*, 7120–7126.
Noller, H., & Bernhard, S. (1965) *Biochemistry 4*, 1118–1126.
Patapoff, T. W., Thomas, G. A., Wang, Y., & Peticolas, W. L. (1988) *Biopolymers 27*, 493–507.
Rettig, W., Wermuth, G., & Lippert, E. (1979) *Ber. Bunsenges. Phys. Chem. 83*, 692 and references therein.
Robertus, J. D., Kraut, J., Richard A. A., & Birktoft, J. J. (1972) *Biochemistry 11*, 4293–4303.
Schechter, I., & Berger, A. (1967) *Biochem. Biophys. Res. Commun. 27*, 157–162.

Schmidt, J., Benecky, M., Kafina, M., Watters, K. L., & McFarland, J. T. (1978) *FEBS Lett. 96*, 263–268.
Schonbaum, G. R., Zerner, B., & Bender, M. L. (1961) *J. Biol. Chem. 236*, 2930.
Singer, P. T., Smalas, A., Carty, R. P., Mangel, W. F., & Sweet, R. M. (1993) *Science 259*, 669–673.
Stoddard, B. L., Bruhnke, J., Porter, N., Ringe, D., & Petsko, G. A. (1990) *Biochemistry 29*, 4871–4879.
Tonge, P. J., & Carey, P. R. (1988) *Proceedings of the Second European Conference on the Spectroscopy of Biological Molecules* (Schmid, E. D., Schneider, F. W., & Siebert, F., Eds.) pp 117–120, Wiley, New York.
Tonge, P. J., & Carey, P. R. (1989) *Biochemistry 28*, 6701–6709.
Tonge, P. J., & Carey, P. R. (1990a) *Proceedings of the Twelfth International Conference on Raman Spectroscopy* (Durig, J. R., & Sullivan, J. F., Eds.) pp 724–725, Wiley, Newq York.
Tonge, P. J., & Carey, P. R. (1990b) *Biochemistry 29*, 10723–10727.
Tonge, P. J., & Carey, P. R. (1992) *Biochemistry 31*, 9122–9125.
Tonge, P. J., Pusztai, M., White, A. J., Wharton, C. W., & Carey, P. R. (1991) *Biochemistry 30*, 4790–4795.
Walsh, C. (1979) *Enzymatic Reaction Mechanisms*, pp 56–97, W. H. Freeman and Company, San Francisco.
Warshel, A., & Russell, S. T. (1984) *Q. Rev. Biophys. 17*, 283–422.
Wells, J. A. (1990) *Biochemistry 29*, 8509–8517.
Wells, J. A., Cunningham, B. C., Graycar, T. P., & Estell, D. A. (1986) *Philos. Trans. R. Soc. London A A317*, 415–423.
Winkler, F. K., D'Arcy, A., & Hunziker, W. (1990) *Nature 343*, 771–774.
Yue, K. T., Deng, H., & Callender, R. (1989) *J. Raman Spectrosc. 20*, 541–545.